Sensors and Actuators B 224 (2016) 654–660

Contents lists available at ScienceDirect

Sensors and Actuators B: Chemical

journal homepage: www.elsevier.com/locate/snb

Low-working-temperature, fast-response-speed NO_2 sensor with nanoporous-SnO_2/polyaniline double-layered film

Hongyan Xu*, Dianxing Ju, Wenru Li, Haibo Gong, Jun Zhang, Jieqiang Wang, Bingqiang Cao*

School of Materials Science and Engineering, Shandong Provincial Key Laboratory of Preparation and Measurement of Building Materials, University of Jinan, No. 336, West Road of Nan Xinzhuang, Jinan 250022, Shandong, China

ARTICLE INFO

Article history:
Received 10 July 2015
Received in revised form 20 October 2015
Accepted 22 October 2015
Available online 25 October 2015

Keywords:
SnO_2 nanoporous material
Polyaniline
Layered double thick film
NO_2 gas sensing

ABSTRACT

A SnO_2/polyaniline (PANI) double-layered film sensor for NO_2 detection was fabricated using nanoporous SnO_2 and PANI layers. The double layered film sensor has high selectivity and high response to NO_2 gas even with low concentration. Furthermore, the double layered film sensor also has a low optimum working temperature (140 °C) and high stability over a long working time period. The response and recovery time of sensor S_5P500 is as short as about 17 s and 25 s to 37 ppm NO_2 at 140 °C, respectively. The experiment results show that the porous characteristics of nanoporous SnO_2 and the thickness of PANI have effect on the sensor response of double layered film sensors. The improved sensing properties mainly attributes to the formation of depletion layer at the p–n junction interface in SnO_2/PANI double layered film sensor, which makes great resistivity difference in air and NO_2 gas. Thus, the combination of n-type SnO_2 thick film and p-type PANI thick film provides an effective strategy to design high property gas sensors.

1. Introduction

NO_2 is a colorless, flammable and hazardous gas, produced in such processes as automobile exhaust, production of nitric acid, and the combustion of coal and fuel [1]. It has also been widely used to promote chemical reactions and rocket fuels because of its high oxidation ability. However, the air pollution caused by nitrogen oxides (NO_2) is becoming a more and more important environmental issue. NO_2 associated with other pollutants like volatile organic compounds (VOC) can lead to the formation of ozone (O_3) in lower atmosphere and smog in urban areas, which is believed to be harmful to the respiratory system of human beings and animals. In addition, NO_2 gas can produce acid rain and damage plants [2,3]. Therefore, it is an urgent work to develop the NO_2 gas sensor with high sensitivity and relatively low working temperature for the atmosphere monitoring.

Semiconducting tin oxide (SnO_2) has been proven to be one of the most attractive sensing materials for gas sensors, owing to its suitable physical–chemical properties, and ability to detect many reducing and oxidizing gases sensitively [4–6]. Till now, a lot of works have been carried out to fabricate NO_2 gas sensor based on tin oxide (SnO_2) thin film. However, most of those sensors with limited sensitivity must work at high temperature (300–450 °C) [7,8]. As we all know, low operating temperature (<200 °C) and high responding rate are two major objectives [3]. Currently, worldwide efforts are concentrated on developing the fast responding and recovery NO_2 gas sensors operated at low temperature [9].

Gas sensors based on polyaniline (PANI) materials have been attracting more attention in recent years [10–13] because of their high sensitivity and unique conductivity properties at low temperature. The high performance originates from its ability to transport charge carriers along the polymer backbone and hop the carriers between polymer chains. Thus PANI molecules can easily react with de-/protonating (reductive and oxidative) agents inducing the change of their conductivity at low temperature. The gas sensing devices based on organic materials, such as PANI and polypyrrole, exhibit high gas sensitivity at lower temperature. It has been reported that organic-inorganic composite materials can synergize or improve the properties of the pure organic or inorganic materials in electronics, coating, optics, catalysis and so on [14–16].

In order to gain better gas sensing properties, we proposed here a new route to prepare nanoporous-SnO_2/PANI double-layered film for sensing applications. The nanoporous SnO_2 can be assumed as a special material, which possesses both high reactivity of nanoparticles and mechanical strength of nanoceramics

* Corresponding authors. Tel.: +86 53189736292; fax: +86 53187974453.
E-mail addresses: mse_xuhy@ujn.edu.cn (H. Xu), mse_caobq@ujn.edu.cn (B. Cao).

http://dx.doi.org/10.1016/j.snb.2015.10.076
0925-4005/

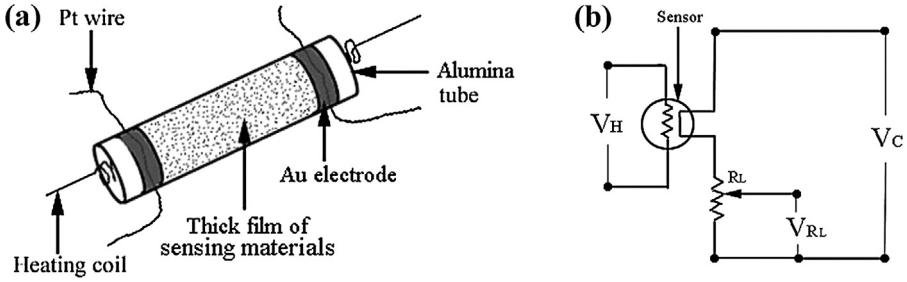

Fig. 1. (a) Schematic drawing of a sensor element. Al_2O_3 tubes (4.0 mm in length, 1.0 mm in internal diameter and 1.4 mm in external diameter) with a pair of Au electrodes (2.0 mm in distance) attached with Pt lead wires. (b) Electric circuit used in the sensor testing equipment. V_H is the heating voltage, R_L is a constant resistance (=1 MΩ), V_{R_L} is the voltage on R_L, V_C is the constant voltage (=5 V) applied on the R_L and the sensor, the signal voltage $V_S = V_C - I_{R_L} \cdot R_s = V_s/I$ is the resistance of the sensor, $R_s = R_a$ (in air) and $R_s = R_g$ (in target gas).

[17–19]. Nanoporous SnO_2 layer is composed of interconnected SnO_2 nanoparticles, which form a framework with numerous pores, and it exhibits higher sensor response and quicker response speed. The SnO_2/PANI double-layered film sensors simply prepared by this new route show the advantages of sensitivity (with a gas response of 8.1 to 37 ppm NO_2 at 140 °C), selectivity, and rapid response for NO_2 gas at the relative low working temperature (140 °C). These characteristics enable it possible to use as a NO_2 gas sensor.

2. Experimental

2.1. Preparation of SnO_2 nanoporous material

The SnO_2 nanoporous material was prepared by a solvo-thermal hot-press (SHP) process, which was conducted in a solvo-thermal hot-press (SHP) autoclave [19]. The starting materials were SnO_2 nanoparticles and dioxane. SnO_2 nanoparticles (with average size of 50–70 nm) were purchased from Luoyang Institute of Materials, Henan, China, and used as received. In a typical process, 6 g of SnO_2 nanoparticles was ground after mixed with dioxane (e.g. 6 ml, 7 ml, 8 ml, 9 ml and 10 ml) in a high-energy ball mill for 4 h with a turning speed of 180 r/min. The pretreated paste was mounted into a SHP autoclave and its temperature was heated to 200 °C from room temperature at a ramping rate of 3 °C/min, during which the pressure in the autoclave was kept at 60 Mpa. After reacting for 90 min, the autoclave was cooled naturally to room temperature. Thus SnO_2 nanoporous material was obtained and named as SnO_2 nanoporous material S_1 to S_5 according to different amount of dioxane addition.

2.2. Preparation of PANI

Aniline (analytical purity) was distilled under reduced pressure and stored at low temperature (0 °C) before used. Analytical grade hydrochloric acid (HCl, 36–38%), ammonium peroxydisulfate (APS, $(NH_4)_2S_2O_8$) were used as received. 0.2 g of aniline (which dispersed in 4 ml 1 M HCl) and 15 ml of anhydrous ethanol were added into a three-neck flask in sequence, sealed, and dispersed by ultrasonic treatment for 5 min. Thereafter the flask was transferred into a thermostatic bath of 0 °C and stirred constantly for 15 min, followed by dropwise addition of precooled APS aqueous solution (15 ml, 0.03 M) within 1 h and maintained at 0 °C for 24 h. The resulting emerald product was collected by filtration. The precipitates were sequentially washed 3 times with distilled water and anhydrous ethanol, and finally dried in a vacuum oven at 50 °C for 12 h.

2.3. Preparation of SnO_2/PANI double-layered film sensors

1 g of SnO_2 nanoporous material S_1 was ground in an agate mortar for 10 min, and 2 ml de-ionized water was added into the agate mortar and grinded for another 10 min. Then, the resultant paste was coated onto the outer surface of an alumina (Al_2O_3) tube (4.0 mm in length, 1.0 mm in internal diameter and 1.4 mm in external diameter) with a pair of Au electrodes (2.0 mm in distance) attached with Pt lead wires, as shown in Fig. 1a. The SnO_2 coated Al_2O_3 tube was sintered at 650 °C in air for 2 h to finish the preparation of SnO_2 nanoporous material film. The preparation process of other SnO_2 nanoporous material thick film (e.g. S_2, S_3, S_4 and S_5) was all the same as S_1.

Finally, PANI paste was acquired by adding 100 mg PANI to 1 ml NMP (*N*-methylpyrrolidone) and fully grounding. PANI paste was coated on the outer surface of SnO_2 porous layer (e.g. S_1, S_2, S_3, S_4 and S_5), respectively. After drying at room temperature in air for 12 h, SnO_2/PANI composite sensors denoted as S_1P100, S_2P100, S_3P100, S_4P100 and S_5P100 were fabricated, respectively.

Furthermore, in order to find the effect of PANI concentration on sensing properties of layered double thick film, PANI paste with different proportions were prepared by adding 10, 50, 100, 200 and 500 mg PANI to 1 ml NMP, respectively. Five concentrations of PANI paste were coated on the outer surface of SnO_2 nanoporous material thick film S_5, respectively. After drying at room temperature in air for 12 h, layered double thick film sensors S_5P10, S_5P50, S_5P100, S_5P200 and S_5P500 were fabricated, respectively. Three sensors of each kind were fabricated by the same procedure.

Pure PANI thick film sensors (denoted as P-0) were also fabricated as a reference using only PANI paste. Unfortunately, the PANI film is so loose to tend to peel off from the Al_2O_3 tube. Therefore its sensor response cannot be obtained.

2.4. Characterization of the samples

The porosity and primary pore diameter of the SnO_2 nanoporous material were examined by BET and BJH methods using a N_2 adsorption isotherm with a Physisorption Analyzer (Micromeritics, ASAP2020). The molecular structures of PANI were measured with a Nicolet NEXUS-670 Fourier-transform infrared (FTIR) spectroscopy with spectral resolution of 4.00 cm^{-1} and wave number precision of 0.01 cm^{-1}. SEM photographs of the thick film were taken with a Hitachi S-2500 scanning electron microscope.

2.5. Gas sensing performance

The sensors performance was tested by a gas sensor measurement system (WS-30A, Weisheng Electronics, Zhengzhou, China). The devices were put into an airproof test box. Prior to the measurement, the sensors were aged at 160 °C for 36 h in air. The electronic circuit used is shown in Fig. 1b. In order to gain the selectivity of sensors to NO_2 gas, the testing gases are NO_2, NH_3, CO, H_2 and ethanol vapors. Test gases such as ethanol with calculated concentration

Table 1
Average pore size, pore volume and surface area of SnO_2 nanoporous material S_1, S_3, S_5.

Sample	Amount of solvent (ml)	Average pore size (nm)	Pore (volume/(cm^3/g))	Surface (area/(m^2/g))
SnO_2 nanoporous material S_1	6	34.9	0.038	4.76
SnO_2 nanoporous material S_3	8	20.6	0.027	8.21
SnO_2 nanoporous material S_5	10	18.6	0.023	7.48

were injected into the testing chamber by a microsyringe. The sensor response to oxidizing gases (e.g. NO_2) is defined as follow: $S = R_g/R_a$, where R_g and R_a are the resistance of the gas sensor in testing gas and in air. While for reducing gases, such as NH_3, CO, H_2 and ethanol vapors, it is defined as follow: $S = R_a/R_g$. The response time is defined as the duration within which the signal voltage reaches 90% of its maximum value when gas is introduced into the chamber, and the recovery time is the interval that the voltage decreases by 90% of its maximum valued. Different concentrations of NO_2 gas were tested in the following sequence, 5, 10, 15, 20, 25, 30, 35, 37 and 50 ppm at a relative humidity (RH) of 15–25%.

3. Results and discussion

3.1. Pore size distribution and specific surface area of nanoporous materials

Table 1 shows pore size distribution and specific surface area of SnO_2 nanoporous material S_1, S_3 and S_5. As shown in Fig. 2, the surface area and the number of nanopores with a size of 2–3 nm in diameter of SnO_2 nanoporous material increased with the increasing dioxane amount. SnO_2 nanoporous material S_3 shows the biggest surface area of 8.21 m^2/g when the amount of dioxane is 10 ml. On the contrary, the average pore size and pore volume decreased with the increase in the amount of dioxane as shown in Table 1. And SnO_2 nanoporous material S_5 has the smallest average pore size of 18.6 nm when the amount of solvent is 10 ml. The above results indicate that the pore properties of nanoporous material obviously change when different amount of dioxane is added into SnO_2 nanoparticles in the preparation process of nanoporous material.

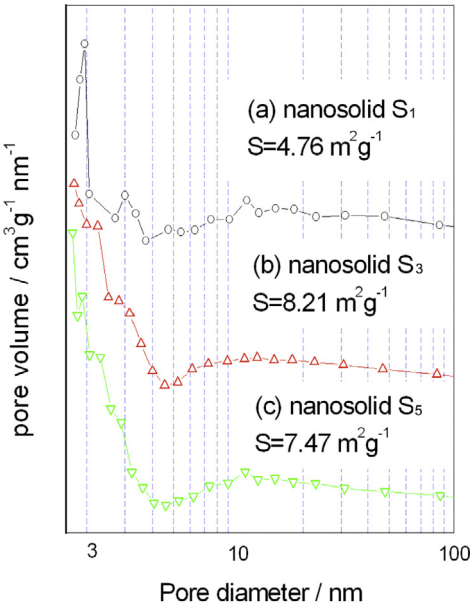

Fig. 2. Pore size distributions of SnO_2 nanoporous material S_1, S_3 and S_5.

3.2. FTIR spectroscopy of PANI

To verify the composition of PANI, we measured the infrared spectrum of the products. The spectral region is from 4000 to 400 cm^{-1}. As shown in Fig. 3, the peak at around 3419 cm^{-1} is due to the stretching vibration of adsorbed H_2O in air. The peaks at 1597, 1554 and 1419 cm^{-1} are assigned to the stretching vibration of C=N along with deforming vibration of N—H [18]. The peak at 1492 cm^{-1} corresponds to the stretching vibration of C=C in benzenoid or quinonoid rings [20–24]. The peaks at 1300 cm^{-1} are attributed to the stretching vibrations of C—N in benzenoid rings [21–23]. The strongest peak centered at 1124 cm^{-1} is due to the in-plane bending vibration of benzenoid or quinonoid C—H [20,21,25,26]. The peaks around 800–687 cm^{-1} can be assigned to the out-of-plane bending vibrations of benzenoid or quinonoid C—H and N—H [20,25,26].

3.3. Morphology of the SnO_2/PANI layered double thick film

Fig. 4a and b shows the surface morphology of SnO_2 nanoporous material thick film S_5 and SnO_2/PANI layered double thick film S_5P500, respectively. It can be seen that the SnO_2 nanoporous material thick film (Fig. 4a) is compact and has strong adhesion with the Al_2O_3 tube substrate. In addition, there are a lot of pores (or channels) in SnO_2 nanoporous material thick film shown in the inset of Fig. 4a, which are greatly beneficial for compounding with polyaniline and improving the sensor response. In the experiment, it was found that pure PANI film is much loose and easy to peel off from the Al_2O_3 tube. Interestingly, when PANI was coated on SnO_2 nanoporous material thick film, the PANI film became more compact than that of being coated on Al_2O_3 tube as shown in Fig. 4c. It may be due to the porous structure of SnO_2 nanoporous material thick films as shown in the inset of Fig. 4a. Moreover, it shows cross-sectional interface of a SnO_2/PANI layered double thick film as shown in Fig. 4c, which clearly indicates the formation of a diffusion free interface. It is evident that there are many pores on the PANI surface, which seem to contribute to short response and recovery times.

3.4. Gas sensing properties of SnO_2/PANI layered double thick film sensors

Fig. 5 shows a relationship between working temperature and sensor response of SnO_2/PANI layered double thick film sensor S_5P100 toward different target gases. The target gases are 1000 ppm CO, 1000 ppm H_2, 1000 ppm ethanol vapor, 10 ppm NO_2 and 10 ppm NH_3. It can be seen clearly from the figure that sensor S_5P100 had comparatively strong response to 10 ppm NO_2, but no response to other gases when the working temperature was lower than 180 °C. While the temperature was higher than 200 °C, the response of sensor to ethanol vapor became stronger than that of sensor to NO_2. In addition, the high response to NO_2 demonstrates the high selectivity for NO_2 gas under an optimum working temperature of 140 °C. This may be due to the formation of p–n junction, which lowers the activation energy and enthalpy of physisorption for vapors with good electron-donating characteristics [27,11]. Moreover, the different reaction activity of target gases in terms of bond energy maybe another reason for the different enhancement of SnO_2/PANI layered double thick films gas sensing property,

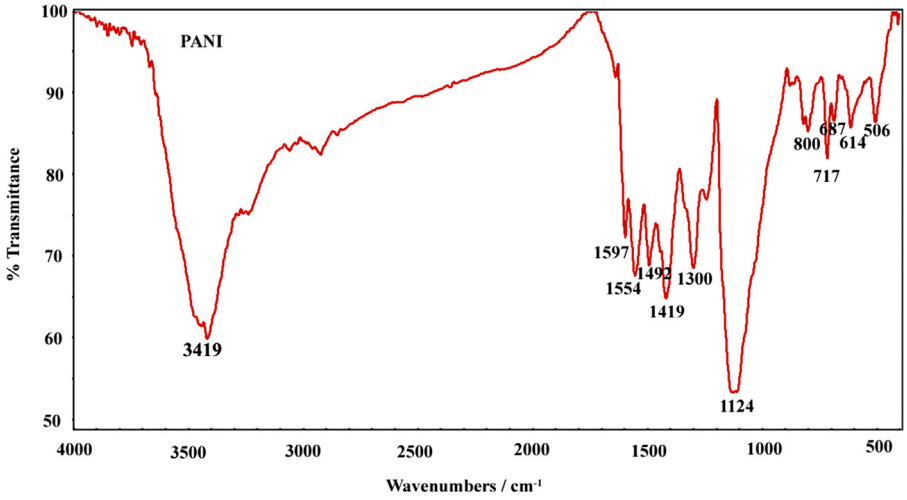

Fig. 3. FTIR spectrum of PANI.

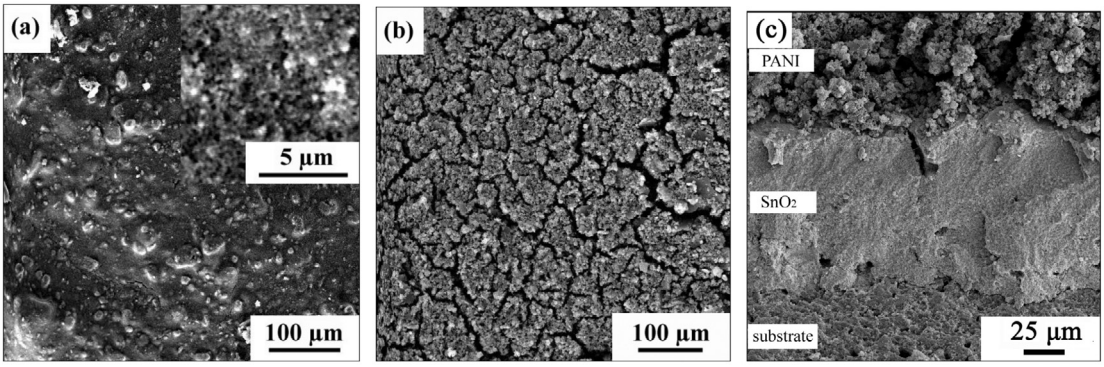

Fig. 4. SEM photographs of (a) SnO_2 nanoporous material thick film S_5 annealed at 650 °C, (b) S_5P500, and (c) an interface cross-section of a SnO_2/PANI layered double thick film S_5P500.

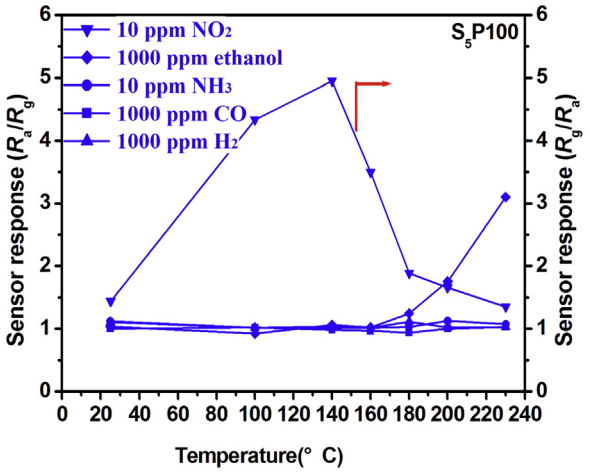

Fig. 5. Relationship between working temperature and sensor response of Sensor S_5P100 to different target gases.

because the bond energy possesses very important influence on the stability/activity of compounds, that is, the lower the bond energy, the easier the bond breaks. Here, the main bond energy of measured target gas, e.g., NO_2 (N—O), ethanol (O—H), NH_3 (N—H), C=O (C≡O) and H_2 (H—H) are 230, 458.8, 386, 1351.7, 432 kJ/mol, respectively [28–30]. It can be found clearly that the bond strength of N—O in NO_2 is the weakest, so NO_2 is the unstablest one in terms of bond energy of all of 5 gases as shown in Fig. 5. Although the actual gas sensing process is significantly complicated, it is most probably that the reasons for the excellent selectivity of our sensor toward NO_2 are the high absorbing ability and the low bond energy of N—O in NO_2.

In order to characterize the formation of p–n heterojunction between the interface of SnO_2 and PANI, the current density–voltage (I–V) characteristics of the films were measured. Supplementary information Fig. S1 shows the change in I–V characteristics of sensors with SnO_2 film and SnO_2/PANI double-layered film. As shown in Fig.S1a, I–V characteristic of SnO_2 film is ohmic, which is linear in the bias range of −2.0 to 2.0 V. However, the I–V characteristic of SnO_2/PANI double-layered film shows diode characteristics as shown in Fig. S2b. These results indicate that p–n junctions have formed between the interface of SnO_2 and PANI.

In order to examine the stability of layered double thick film sensors to NO_2 over a longer working time period, the performance of sensor S_5P500 and S_5P100 were continuously monitored for 18 min. Fig. 6 shows typical response profiles of two kinds of gas sensors to 37 ppm of NO_2 at 140 °C. These two kinds of sensors exhibit a reproducible run after four cycles, which demonstrates good device repeatability.

As same as stability, the response/recovery time is an important parameter used for characterizing a sensor performance. According to the definition of response and recovery time, it can also be clearly observed from Fig. 6 that when the target gas was injected into the box, both of the two sensors response fast and the response time of sensor S_5P100 and S_5P500 is 14 and 17 s, respectively. After evacuation, sensor S_5P500 needs 25 s to recover to a low resistance state which is longer than that of sensor S_5P100 (20 s). To our

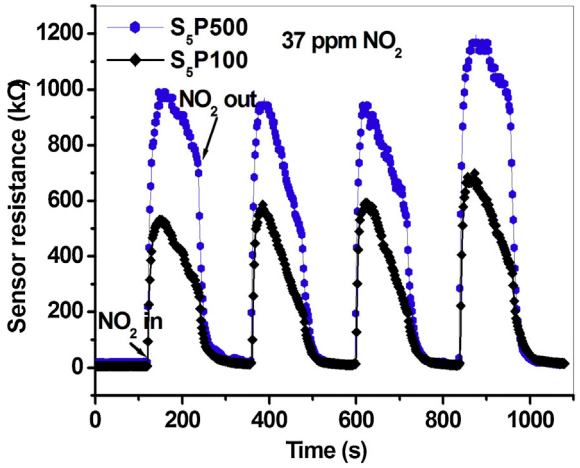

Fig. 6. Sensing performance of Sensor S_5P500 and S_5P100 at 140 °C over a longer working time period. The target gas is NO_2 with a concentration of 37 ppm.

knowledge, no other methods were used to synthesize PANI or SnO_2/PANI layered double thick film with a more rapid response and recovery speed to NO_2 gas as reported in literature. For example, in 2007, Yan et al. [10] synthesized polyaniline nanofibers to detect NO_2, and the response time (when $R/R_0 = 10$) of polyaniline nanofiber sensor to 50 ppm NO_2 is 173 s at room temperature. In 2011, Sharma et al. [31] synthesized SnO_2 thin films using RF sputtering technique and the response and recovery time of SnO_2 thin film to 50 ppm NO_2 was a few minutes and a few tens of minutes at 140 °C, respectively. Compared with the above mentioned, our SnO_2/PANI layered double thick film have more rapid response and recovery speed. This may be due to the porous structure of SnO_2 nanoporous material and PANI thick film as shown in Fig. 4c. Due to the porous structure, NO_2 diffusion as well as reaction between gas molecules and the interface occurs more easily. Our experimental results indicate that the SnO_2/PANI layered double thick film sensors with rapid response and recovery speed are quite stable and can be used as recyclable NO_2 sensors.

Fig. 7a shows the relationship between working temperature and sensor response of SnO_2/PANI layered double thick film sensors S_1P100, S_2P100, S_3P100, S_4P100 and S_5P100 to 37 ppm NO_2. It can be seen that sensor S_5P100 has the highest response when the working temperature was lower than 140 °C, which indicated that the pore properties (shown as Table 1) of SnO_2 nanosolid surely have effect on improving the response of SnO_2/PANI layered double thick film to NO_2. It should be mentioned that we investigated the sensing response of pure SnO_2 thick films exposed to 37 ppm NO_2 at 140 °C as well. However, the results show that the resistance is so high that we cannot observe the sensor response at 140 °C. It may be due to the working temperature (140 °C) is much lower to pure SnO_2 thick films.

The relationship between working temperature and sensor response of SnO_2/PANI layered double thick film sensors S_5P10, S_5P50, S_5P100, S_5P200 and S_5P500 to 37 ppm NO_2 have been shown in Fig. 7b. It can be seen that S_5P500 has the highest response when the working temperature is higher than 100 °C, and its optimum working temperature is 140 °C. Moreover, with the increasing amount of PANI in layered double thick film, the sensor response became stronger and stronger in almost all working temperature range. It indicated that the content of PANI have great effect on the response of that sensors to NO_2.

Experiments have been carried out for SnO_2/PANI layered double thick film sensor S_5P10, S_5P50, S_5P100, S_5P200 and S_5P500 for the gas sensor response of NO_2 under the different gas concentrations at 140 °C. It can be clearly observed from Fig. 8 that all sensors

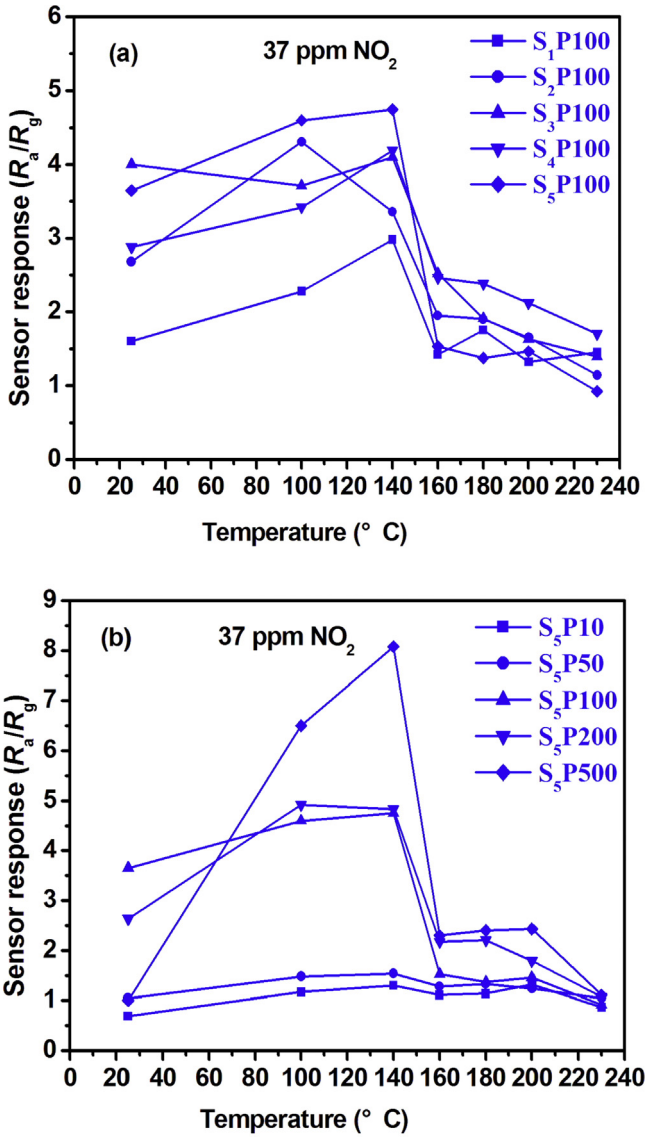

Fig. 7. Relationship between working temperature and sensor response of sensors to 37 ppm NO_2 (a) S_1P100, S_2P100, S_3P100, S_4P100 and S_5P100, (b) S_5P10, S_5P50, S_5P100, S_5P200 and S_5P500.

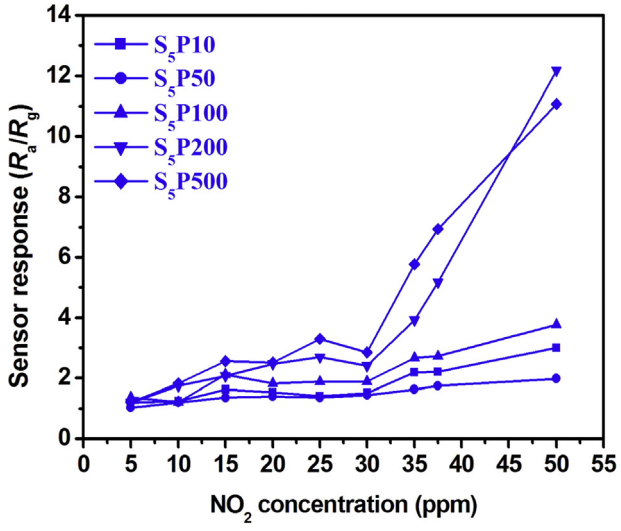

Fig. 8. Relationship between sensor response and NO_2 concentration of Sensors S_5P10, S_5P50, S_5P100, S_5P200 and S_5P500 at 140 °C.

show good dependence on NO_2 concentrations. The effects of PANI content on its gas sensing properties are also obvious. It should be mentioned that we prepared layered double thick film sensor from higher PANI content as well. But it was found that the PANI thick film became easy to peel off when the PANI content in PANI together NMP paste is more than 50%. Therefore, the PANI content cannot be too high in our experiments.

In addition, in order to investigate the effect of moist to the gas sensing performance of sensors, some experiments in different relative humidity have been carried out. The results demonstrate that there is little effect of the gas sensing performance of S_5P500 with the low relative humidity of 11% RH and the high relative humidity of 28% RH, as shown in Supplementary information Fig. S2a and b, respectively.

3.5. *Mechanism of the enhanced sensing properties SnO_2/PANI layered double thick film*

As shown in Fig. 6, on exposure to oxidizing NO_2 gas SnO_2/PANI layered double thick film sensors shows sharply increase in the resistance. On the contrary, the sensor resistance of S_5P500 decreases when exposed to ethanol as shown as Fig. S3 in Supplementary information. The SnO_2/PANI double-layered film sensors prepared by us show different directions of resistance changes to NO_2 and ethanol gas. This indicates the n-type behavior and therefore charge transport is mainly through SnO_2. The sensing mechanism of n-type semiconductor sensors has been put forwarded by some papers. For SnO_2 based sensing materials, the mechanism can be explained by the space-charge layer mode [32–34]. When the SnO_2 are exposed to fresh air at a high temperature, oxygen molecules will be adsorbed on the SnO_2 surface and extract electrons to form oxygen ions species (O_2^-, O^{2-}, or O^-) and further cause the formation of depletion layers in the surface of SnO_2 based sensing materials [32–34]. As a result, the formation of depletion layer decreases the carrier concentration of the materials and leads to a high resistance of the sensor. When the SnO_2 nanoporous material thick film are exposed to NO_2, the NO_2 molecules react with the oxygen ions and extract electrons from depletion layer of SnO_2, which decrease the carrier concentration of SnO_2 and the conductivity of the SnO_2 nanoparticles. However, after been covered by PANI, the mechanism will be different.

SnO_2 is an n-type semiconductor, and PANI a p-type, therefore there are two competitive mechanisms of electronic properties in the SnO_2/PANI layered double thick film. Fig. 9a is the energy band structure diagram of p-type PANI/n-type SnO_2 hetero-contact. It has been known that SnO_2 shows n-type conductivity by electrons and PANI displays p-type conductivity by holes. After PANI are layered with SnO_2 nanoparticles, the p–n junction will be formed between the interface of PANI and SnO_2 nanoparticles, leading to an energy band bending in the depletion layers. Then, the electrons of n-type SnO_2 transfer to p-type PANI and the holes of p-type PANI transfer to n-type SnO_2 until the Fermi levels (E_F) gets equalization, causing a wider depletion layers and increasing the sensor resistance. When PANI/SnO_2 hetero-junction sensor is exposed to air at a high temperature, a depletion layer at their interface will form which make sensor's resistance increase in air as shown in Supplementary information Fig. S4. In addition, the formation of depletion layer on the surface of SnO_2 and PANI lead to the high resistance state of sensing materials, due to the adsorption of oxygen molecules, as shown in Fig. 9b. Fig. 9c exhibits a model for PANI/SnO_2 hetero-junction sensor when exposed to NO_2 gas. As an oxidizing gas, NO_2 molecules will react with the oxygen ions on the surface of SnO_2 nanoparticles and extract the electrons from the SnO_2. Then, NO_2 gas combine with the holes in p-type PANI and produce a NO_x. Because of the above, the potential barrier height and the resistance will be further increased, which show an increase of

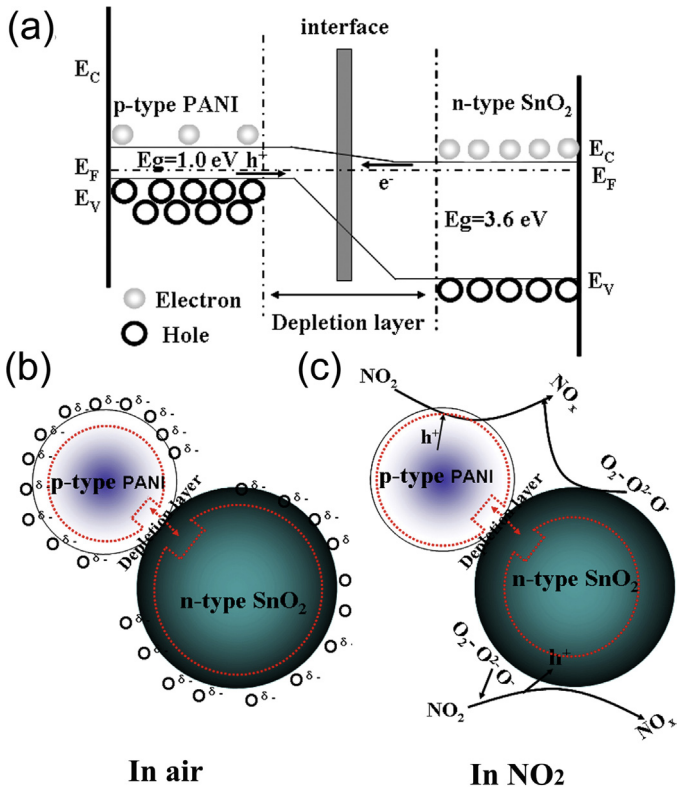

Fig. 9. (a) The energy band structure diagram of n-type SnO_2/p-type PANI heterocontact. (b and c) Schematic model for the n-type SnO_2/p-type PANI heterojunctions based sensor when exposed to air and NO_2 gas, respectively.

response ($S = R_a/R_g$). In a word, the enhanced response to NO_2 for SnO_2/polyaniline double-layered film sensor is mainly attributed to the variation of resistance caused by the formation of p–n junction. This theoretical model can also be used to interpret other systems with their response to oxidizing gas (such as NO_2) improved by p–n junction.

4. Conclusions

In summary, an inorganic/organic SnO_2/PANI double-layered sensor was prepared using a novel SnO_2 nanoporous material and PANI. The sensors exhibit much high response and selectivity to low concentration of NO_2 gas at low working temperature (140 °C) and the response/recovery time are a few seconds and a few tens of seconds, respectively, which overcome the shortcomings of long response time of PANI and the high working temperature of SnO_2. The enhanced response to NO_2 is mainly attributed to the variation of resistance caused by the formation of p–n junction. This theoretical model was further proved by optimization of SnO_2/PANI heterostructure and can also be used to explain other heterojunctions for sensor application. Moreover, to our knowledge, most of semiconductor metal oxide (such as SnO_2, ZnO, Fe_2O_3) nanoporous material can be prepared by the solvothermal hot-press (SHP) process. Furthermore, the nanoporous material can be well compounded with organic material. Therefore this novel method possesses a wide versatility, which makes it possible to develop other new kinds of chemical gas sensors.

Acknowledgements

This work is supported by National Natural Science Foundation of China (NSFC, No. 60906008), Shan-dong Provincial Science

Foundation (No. ZR2014JL045 and ZR2015BQ006) and Science Foundation of University of Jinan (No. XKY1504).

Appendix A. Supplementary data

Supplementary data associated with this article can be found, in the online version, at http://dx.doi.org/10.1016/j.snb.2015.10.076.

References

[1] B.T. Marquis, J.F. Vetelino, A semiconducting metal oxide sensor array for the detection of NO_x and NH_3, Sens. Actuators, B: Chem. 77 (2001) 100–110.
[2] J. Brunet, V.P. Gracia, A. Pauly, C. Varenne, B. Lauron, An optimised gas sensor microsystem for accurate and real-time measurement of nitrogen dioxide at ppb level, Sens. Actuators, B: Chem. 134 (2008) 632–639.
[3] A. Sharma, M. Tomar, V. Gupta, Enhanced response characteristics of SnO_2 thin film based NO_2 gas sensor integrated with nanoscaled metal oxide clusters, Sens. Actuators, B: Chem. 181 (2013) 735–742.
[4] H.Y. Xu, X.Q. Chen, J. Zhang, J.Q. Wang, B.Q. Cao, D.L. Cui, NO_2 gas sensing with SnO_2–ZnO/PANI composite thick film fabricated from porous nanosolid, Sens. Actuators, B: Chem. 176 (2013) 166–173.
[5] K.M. Kim, K.I. Choi, H.M. Jeong, H.J. Kim, H.R. Kim, J.H. Lee, Highly sensitive and selective trimethylamine sensors using Ru-doped SnO_2 hollow spheres, Sens. Actuators, B: Chem. 166–167 (2012) 733–738.
[6] I.S. Hwang, S.J. Kim, J.K. Choi, J.J. Jung, D.J. Yoo, K.Y. Dong, B.K. Ju, J.H. Lee, Large-scale fabrication of highly sensitive SnO_2 nanowire network gas sensors by single step vapor phase growth, Sens. Actuators, B: Chem. 165 (2012) 97–103.
[7] Z. Ling, C. Leach, The effect of relative humidity on the NO_2 sensitivity of a SnO_2/WO_3 heterojunction gas sensor, Sens. Actuators, B: Chem. 102 (2004) 102–106.
[8] A.A. Firooz, T. Hyodo, A.R. Mahjoub, A.A. Khodadadi, Y. Shimizu, Synthesis and gas-sensing properties of nano- and meso-porous MoO_3-doped SnO_2, Sens. Actuators, B: Chem. 147 (2010) 554–560.
[9] N. Dewan, S.P. Singh, K. Sreenivas, V. Gupta, Influence of temperature stability on the sensing properties of SAW NO_x sensor, Sens. Actuators, B: Chem. 124 (2007) 329–335.
[10] X.B. Yan, Z.J. Han, Y. Yang, B.K. Tay, NO_2 gas sensing with polyaniline nanofibers synthesized by a facile aqueous/organic interfacial polymerization, Sens. Actuators, B: Chem. 123 (2007) 107–113.
[11] L.N. Geng, Y.Q. Zhao, X.L. Huang, S.R. Wang, S.M. Zhang, S.H. Wu, Characterization and gas sensitivity study of polyaniline/SnO_2 hybrid material prepared by hydrothermal route, Sens. Actuators, B: Chem. 120 (2007) 568–572.
[12] I. Fratoddi, I. Venditti, C. Cametti, M. Vittoria Russo, Chemiresistive polyaniline-based gas sensors: a mini review, Sens. Actuators, B: Chem. 220 (2015) 534–548.
[13] G. Ćirić-Marjanović, Recent advances in polyaniline research: polymerization mechanisms, structural aspects, properties and applications, Synth. Met. 177 (2013) 1–47.
[14] M. Satoshi, N. Hiroyoshi, K. Yoshihiko, M. Yukihito, M. Kimihiro, Photocarrier generation at nano-interfaces in organic polysilane–titania matrix hybrid thin films, Thin Solid Films 438–439 (2003) 253–256.
[15] J.G. Magdalena, L.O. Duan, O. Brmsby, C.S. Alice, R.H.W. John, A new solid acid catalyst: the first phosphonate and phosphonic acid functionalized microporous polysilsesquioxanes, Chem. Commun. 1 (2001) 67–68.
[16] D.S. Dhawale, R.R. Salunkhe, U.M. Patil, K.V. Gurav, A.M. More, C.D. Lokhande, Room temperature liquefied petroleum gas (LPG) sensor based on p-polyaniline/n-TiO_2 heterjunction, Sens. Actuators, B: Chem. 134 (2008) 988–992.
[17] H. Xu, X. Liu, M. Li, Z. Chen, D. Cui, M. Jiang, X. Meng, L. Yu, C. Wang, Preparation and characterization of TiO_2 bulk porous nanosolid, Mater. Lett. 59 (2005) 1962–1966.
[18] X. Liu, L. Yu, H. Xu, M. Li, C. Wang, M. Jiang, D. Cui, Degradation of RhB catalyzed by TiO_2 bulk porous nanosolid, Acta Chim. Sin. 62 (2004) 2398–2402.
[19] H.Y. Xu, X.L. Liu, D.L. Cui, M. Li, M.H. Jiang, A novel method for improving the performance of ZnO gas sensors, Sens. Actuators, B: Chem. 114 (2006) 301–307.
[20] L.G. Gai, G.J. Du, Z.Y. Zuo, Y.M. Wang, D. Liu, H. Liu, Controlled synthesis of hydrogen titanate–polyaniline composite nanowires and their resistance–temperature characteristics, J. Phys. Chem. C 113 (2009) 7610–7615.
[21] C.Q. Bian, Y.J. Yu, G. Xue, Synthesis of conducting polyaniline/TiO_2 composite nanofibres by one-step in situ polymerization method, J. Appl. Polym. Sci. 104 (2007) 21–26.
[22] H. Liu, J.Y. Wang, X.B. Hu, R. Boughton, S.R. Zhao, Q. Li, M.H. Jiang, Structure and electronic transport properties of polyaniline/$NaFe_4P_{12}$ composite, Chem. Phys. Lett. 352 (2002) 185–190.
[23] N. Parvatikar, S. Jain, C.M. Kanamadi, B.K. Chougule, S.V. Bhoraskar, M.V. Ambika Prasad, Humidity sensing and electrical properties of polyaniline/cobalt oxide composites, J. Appl. Polym. Sci. 103 (2007) 653–658.
[24] Y. Qiu, L. Gao, Novel polyaniline/titanium nitride nanocomposite: controllable structures and electrical/electrochemical properties, J. Phys. Chem. B 109 (2005) 19732–19740.
[25] L.X. Zhang, P. Liu, Z.X. Su, Preparation of PANI–TiO_2 nanocomposites and their solid-phase photocatalytic degradation, Polym. Degrad. Stab. 91 (2006) 2213–2219.
[26] H. Liu, X.B. Hu, J.Y. Wang, R.I. Boughton, Structure, conductivity, and thermopower of crystalline polyaniline synthesized by the ultrasonic irradiation polymerization method, Macromolecules 35 (2002) 9414–9419.
[27] P.J. Benjamin, E. Phillip, J.E. Richard, L.H. Colin, M.R. Norman, Novel composite organic–inorganic semiconductor sensors for the quantitative detection of target organic vapours, J. Mater. Chem. 6 (1996) 289–294.
[28] M. Nie, Organic Chemistry, Metallurgical Industry Press, Beijing, 2008.
[29] X. Cao, T. Song, X. Wang, Inorganic Chemistry, third ed., Higher Education Press, Beijing, 1994.
[30] L.X. Zhang, J.H. Zhao, H.Q. Lu, L. Li, J.F. Zheng, J. Zhang, H. Li, Z.P. Zhu, Highly sensitive and selective dimethylamine sensors based on hierarchical ZnO architectures composed of nanorods and nanosheet-assembled microspheres, Sens. Actuators, B: Chem. 171–172 (2012) 1101–1109.
[31] A. Sharma, M. Tomar, V. Gupta, SnO_2 thin film sensor with enhanced response for NO_2 gas at lower temperatures, Sens. Actuators, B: Chem. 156 (2011) 743–752.
[32] Z.P. Li, Q.Q. Zhao, W.L. Fan, J.H. Zhan, Porous SnO_2 nanospheres as sensitive gas sensors for volatile organic compounds detection, Nanoscale 3 (2011) 1646–1652.
[33] H.C. Chiu, C.S. Yeh, Hydrothermal synthesis of SnO_2 nanoparticles and their gas-sensing of alcohol, J. Phys. Chem. C 111 (2007) 7256–7259.
[34] Y.J. Chen, L. Yu, D.D. Feng, M. Zhuo, M. Zhang, E.D. Zhang, Z. Xu, Q.H. Li, T.H. Wang, Superior ethanol-sensing properties based on Ni-doped SnO_2 p–n heterojunction hollow spheres, Sens. Actuators, B: Chem. 166–167 (2012) 61–67.

Biographies

Hongyan Xu received her Ph.D. degree from State Key Lab of Crystal Materials, Shandong University in 2006. Now she is an Associate Professor at School of Materials Science and Engineering, University of Jinan. Her main research interests are the synthesis and fabrication of semiconductor nano-materials and high performance conductive polymer composite chemical gas sensors.

Dianxing Ju is a graduate student focusing on ZnO semiconductor gas sensor for master degree at University of Jinan. He was awarded a B.Sc. degree in materials science and engineering from the same university in 2012.

Wenru Li graduated from school of materials science and engineering, University of Jinan in 2015. Now he is a graduate student focusing on gas sensing materials for master degree the same university.

Haibo Gong graduated from State Key Lab of Crystal Materials, Shandong University in 2010 and received his Ph.D. degree. Now he is working at School of Materials Science and Engineering, University of Jinan. His main research interests include the fabrication of semiconducting oxide thin films and their applications in light-emitting diodes and the third generation solar cells.

Jun Zhang received his Ph.D. degree from the Department of Chemistry, Nankai University in 2011. Now he is working at School of Materials Science and Engineering, University of Jinan. His research is focused on gas sensing materials.

Jieqiang Wang graduated from Northeastern University in 1999 and received his Ph.D. degree. Now he is a Professor at School of Materials Science and Engineering, University of Jinan. His main research interests are the synthesis and fabrication of semiconductor nano-materials.

Bingqiang Cao is a Professor with Taishan Scholar Chair for material physics with University of Jinan. His research group focuses on semiconducting oxide thin films, heterostructures, nanostructures, and related devices.